Ain Shams Engineering Journal (2018) 9, 1131–1140

Ain Shams University

Ain Shams Engineering Journal

www.elsevier.com/locate/asej
www.sciencedirect.com

MECHANICAL ENGINEERING

Papaya peel extract as potential corrosion inhibitor for Aluminium alloy in 1 M HCl: Electrochemical and quantum chemical study

Namrata Chaubey [a], **Vinod Kumar Singh** [a], **M.A. Quraishi** [b,*]

[a] *Department of Chemistry, Udai Pratap Autonomous College, Varanasi 221002, India*
[b] *Department of Chemistry, Indian Institute of Technology (Banaras Hindu University), Varanasi 221005, India*

Received 5 November 2015; accepted 19 April 2016
Available online 12 July 2016

KEYWORDS

Aluminium alloy;
EIS;
Corrosion inhibition;
SEM;
AFM

Abstract This paper deals with the corrosion inhibition effect of *Papaya peel extract* (PPE) on Aluminium alloy (AA) in 1 M HCl. The corrosion tests were performed by using electrochemical impedance spectroscopy (EIS) and potentiodynamic polarization techniques (PDP). Maximum inhibition efficiency observed is 95.5% and 98.1% from EIS plot and PDP studies at higher concentration (2.0 g L^{-1}) of PPE. Potentiodynamic polarization result shows mainly the cathodic type inhibition for PPE. Surface morphology of AA is carried by scanning electron microscopy (SEM) and atomic force microscopy (AFM). Quantum chemical study is complemented well with the experimental findings of the corrosion inhibition.
© 2016 Ain Shams University. Production and hosting by Elsevier B.V. This is an open access article under the CC BY-NC-ND license (http://creativecommons.org/licenses/by-nc-nd/4.0/).

1. Introduction

Aluminium is known as the second largest attractive materials next to the iron because of having broad application in domestic as well as in industrial process such as automotive, aerospace, construction and electrical power generation. Because of its vast application in daily life, there is much interest to study the electrochemical behaviour of AA. Corrosion resistance behaviour towards a wide variety of corrosive environments is a unique characteristic of AA and this is attributed to the formation of a protective, tightly adhered invisible oxide film on the metal surface. However, dissolution of this protective oxide layer occurs when exposed in acidic or alkaline conditions, due to amphoteric nature of aluminium, yielding Al^{3+} (trivalent aluminium) ions in the acid and AlO_2^- (aluminate) ions in the alkaline medium [1]. HCl is widely used for acid cleaning and electro-polishing of aluminium but it shows strong (pitting) corrosiveness on Al in contact with chlorides [2]. Therefore, it is necessary to add inhibitors to prevent metal corrosion as well as acid consumption. Most well-known inhibitors are organic compounds specially those, containing nitrogen, sulphur, and oxygen atoms and thus showed adsorption on the metal surface. Up to now, various organic compounds are reported as good corrosion inhibitors for

* Corresponding author. Tel.: +91 9307025126; fax: +91 542 2368428.
E-mail addresses: maquraishi.apc@itbhu.ac.in, maquraishi@rediffmail.com (M.A. Quraishi).
Peer review under responsibility of Ain Shams University.

Production and hosting by Elsevier

http://dx.doi.org/10.1016/j.asej.2016.04.010
2090-4479 © 2016 Ain Shams University. Production and hosting by Elsevier B.V.
This is an open access article under the CC BY-NC-ND license (http://creativecommons.org/licenses/by-nc-nd/4.0/).

aluminium in HCl solution [3–7]. But, most of these inhibitors are synthetic chemicals owing to their harmful effect on the environment.

In view of this, it is necessary to develop environmentally safe corrosion inhibitor for aluminium in acidic medium; thus, we have chosen plant extracts as environmentally safe inhibitors that can be extracted using simpler techniques with low cost. The photochemical (includes alkaloids, flavonoids) present in plant extract contains heteroatoms such as N, S, O and π-electrons, aromatic ring, through which they adsorb on metal surface and inhibit corrosion [8]. Recently, most of the plant extracts have been proved to be good inhibitors for aluminium acidic corrosion [9–13]. In that case, by using peel extract as inhibitor is one of the cheap and best option.

There are few reports available on fruit peels as inhibitors for different metals in HCl and H_2SO_4 solutions [14–16]. On the other hand, only Red onion skin extract and ethanolic extracts of Mango peel were studied for aluminium corrosion in hydrochloric acid [17,18]. They showed their maximum inhibition efficiency (η %) in the range of 57.09–88% at higher concentration. In continuation of our work on the development of environmentally benign inhibitors with high effectiveness we have selected Papaya peel and its protection is 94.4% at higher concentration in the present study.

Papaya (Carica papaya) is a common fruit which is grown all over the tropical world and it is used for various health benefits. Peels of papaya fruits are known for their proteolytic activities and are excellent source of papain enzyme which is known to be a major component of papaya peels [19]. Papain is an endolytic cysteine protease. However, Peel of this fruit is generally discarded from home, restaurants and industries. Therefore, the possibility of using industrial waste as corrosion inhibitor is quite interesting from the standpoint of economics and the environment.

The present paper is focused on papaya peel to evaluate their inhibition effect on the corrosion behaviour of an amphoteric metal by means of electrochemical approaches based on potentio-dynamic and electrochemical impedance measurements. Quantum chemical and surface morphological studies are also discussed. There is no report available on papaya peel extract as corrosion inhibitor in HCl and it is first time evaluated in our laboratory.

2. Experimental section

2.1. Materials and chemicals

The corrosion test was performed on AA specimen having the composition in Table 1. Aluminium alloy coupons were purchased from the shop and analysed it in the department of Metallurgical Engineering, IIT (BHU). Stock solution of 1 M HCl was prepared by diluting 37% HCl with double distilled water.

2.2. Inhibitor preparation

Peels were collected from the fruits of Carica papaya and then cleaned with tap water, dried at 50 °C in oven, grind to powdered form. 5 g of powder was taken in 500 ml of 1 M HCl solution and refluxed for 5 h. Thereafter, the mixture was cooled and filtered. The precipitate was dried and weighed. The volume of the filtrate solution was maintained up to 1000 mg L^{-1}. Peels extract test solution was prepared at concentrations of 0.1, 0.5, 1.0 and 2.0 g L^{-1}.

2.3. Electrochemical measurement

The electrochemical measurement was carried out by using Gamry Potentiostat/Galvanostat (Model 300) at room temperature connected with three electrode cells. AA with 1 cm^2 area was used as a working electrode. A platinum foil and a saturated calomel electrode (SCE) i.e. (Cl^-|(4 M) Hg_2Cl_2 (*s*)|Hg (*l*)|Pt) were used as counter and reference electrodes respectively. Gamry application with Echem Analyst version 5.0 software packages was used to analyse the data; all the tests were performed in the absence and presence of different concentrations of PPE. A stabilization period of 30 min immersion was taken before starting the experiment and its open circuit potential (OCP) was recorded as a function of time for 200 s to obtain steady state OCP which corresponds to corrosion potential.

Impedance measurements were carried out in the frequency range 100,000–0.01 Hz using AC signals of amplitude 10 mV peak to peak at open circuit potential. Finally, potentiodynamic polarization curves were obtained by shifting the electrode potential automatically from −0.25 V to +0.25 V vs. OCP at a scan rate of 1 mV/s. To obtain the corrosion current densities (i_{corr}), the extrapolation of the anodic and cathodic curves of the linear Tafel plots are required.

2.4. Surface analysis

The surface study of AA coupons of size 2 × 2.5 × 0.046 cm was analysed by Scanning electron microscope (SEM) and Atomic force microscope (AFM) by immersing in 1 M HCl in the absence and presence of PPE for 3 h at 303 K. The AA strips were taken out from the test solution, washed with distilled water, and dried at room temperature. After drying, coupons were mechanically cut into 1 cm^2 dimensions and then investigated using SEM at an accelerating voltage of 5000 V and 5KX magnification using FEI Quanta 200F microscope and AFM techniques using NT-MDT multimode, Russia, controlled by solver scanning probe microscope controller.

2.5. Quantum chemical study

Quantum chemical study was carried out by using density function theory (DFT) method, B3LYP with electron basis

Table 1 Chemical composition (wt%) of the AA used.

Si	Fe	Cu	Mn	Mg	Zn	Cr	Ti	V	Ga	Al
0.77	0.93	0.02	0.11	0.01	0.01	0.05	0.02	0.01	0.01	Balanced

set 6-31G* (d, p) for all atoms. All the calculations were made with the help of Gaussian 03, E.01 software package [20]. Optimized structures of molecule were obtained with Gaussian 03, E.01m. The quantum chemical parameters obtained were E_{HOMO}, E_{LUMO}, E_{LUMO}–E_{HOMO} (ΔE), total energy and Mulliken charges on heteroatoms (N, O).

3. Results and discussion

3.1. Tafel polarization study

Tafel polarization curves for AA in 1 M HCl at different concentrations of PPE are shown in Fig. 1. The study involves in changing the potential of the working electrode and monitoring the current that is produced as a function of time or potential. As can be seen in Fig. 1, a prominent decrease in the corrosion rate is observed in the presence of PPE, which can be explained by the shifting of cathodic curves to lower values of current densities. However, anodic reaction of corrosion process is slightly inhibited with PPE.

Electrochemical parameters are associated with polarization measurements (Table 2) such as corrosion potential (E_{corr}), corrosion current density (i_{corr}) and cathodic Tafel constants (β_c), values are given in Table 2.

The η % using values of i_{corr} were calculated by following equation:

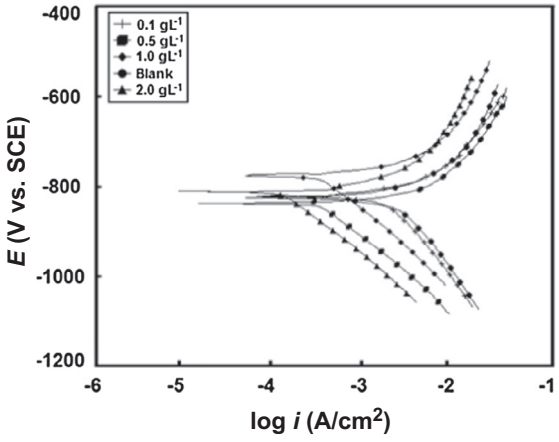

Figure 1 Tafel curves for aluminium in 1 M HCl in the absence and presence of different concentrations of PPE at 303 K.

Table 2 Potentiodynamic polarization parameters for AA in 1 M HCl in the absence and presence of different concentrations of PPE at 300 K.

Inhibitor (g L^{-1})	Tafel polarization			
	i_{corr} (mA cm^{-2})	E_{corr} (mV/SCE)	β_c (mV/dec)	η (%)
Blank	75.6	−818	249	–
0.1	12.7	−776	150	83.2
0.5	8.6	−838	159	88.0
1.0	3.5	−831	147	95.9
2.0	1.4	−859	171	98.1

$$\eta\ \% = \frac{i^0_{corr} - i_{corr}}{i^0_{corr}} \times 100 \quad (1)$$

where i^0_{corr} and i_{corr} are the corrosion current density without and with inhibitor.

The cathodic polarization curves give rise to linear Tafel lines, indicating that the hydrogen evolution reaction is activation controlled. Accordingly, the corrosion current density values are estimated accurately by extrapolating the cathodic linear region back to the corrosion potential. Similar fitting method has been shown by some organic inhibitors for aluminium in HCl [21,22]. But, in anodic domain, it is difficult to recognize the linear Tafel region because PPE retards the anodic reaction slightly of the corrosion process in HCl solution. This result indicates that PPE mainly acts as a cathodic type inhibitor. Furthermore, the parallel cathodic polarization curves suggest that the presence of PPE does not alter the mechanism of hydrogen evolution reaction.

The result shows that the i_{corr} value is higher in HCl but with increasing the concentration of PPE, decrease in i_{corr} and increase in η % occurs and it may be due to the adsorption of inhibitor molecule on metal/acid interface. The maximum decrease in i_{corr} value (1.4 mA cm^{-2}) and maximum η % (98.1) are observed at 2.0 g L^{-1} which confirms that PPE is more efficient inhibitor for aluminium in acid solution.

From the table, it is observed that the presence of PPE shifts E_{corr} to more negative direction with slightly changed its values and also shows an effective change in value of cathodic Tafel constant at different concentrations. From this observation, it can be concluded that PPE can be arranged as a cathodic-type inhibitor [23].

3.2. Electrochemical impedance measurement

EIS is the best technique to giving information about resistive and capacitive behaviour of the interface and also to evaluating the effect of PPE on AA corrosion in HCl. Impedance spectra are recorded and displayed in the form of Nyquist plot (Fig. 2a). Nyquist plot contains two time constant: a capacitive time constant at high frequencies and an inductive time constant at low frequencies. A small diameter is observed in uninhibited system but as the concentration of PPE increases, diameter becomes larger due to increasing resistance. The capacitive time constant originates due to the charge transfer process based on either the conduction of electron through the surface film or direct electron transfer at the metal surface. It is well said that the first time constant is explained in association with electric double layer and charge transfer resistance because of the dielectric properties of a surface layer; i.e. [metal-oxide–hydroxide-inhibitor]$_{ads}$ complex [24].

However, an inductive time constant arises because of adsorbed charged intermediates [25]. When the intermediates are strongly adsorbed, more pronounced spectra are observed. Lenderink et al. [26] have attributed the phenomenon to the relaxation of adsorbed species like H^+_{ads}. However, some authors believed that relaxation adsorbed intermediates include Cl^- [27], oxygen ion [28] or inhibitor species [29] on the electrode surface. Inductive behaviour may also be observed either for the pitted active state and attributed to the surface area modulation and salt film property modulation or due to re-dissolution of the oxide layer surface [30] at low

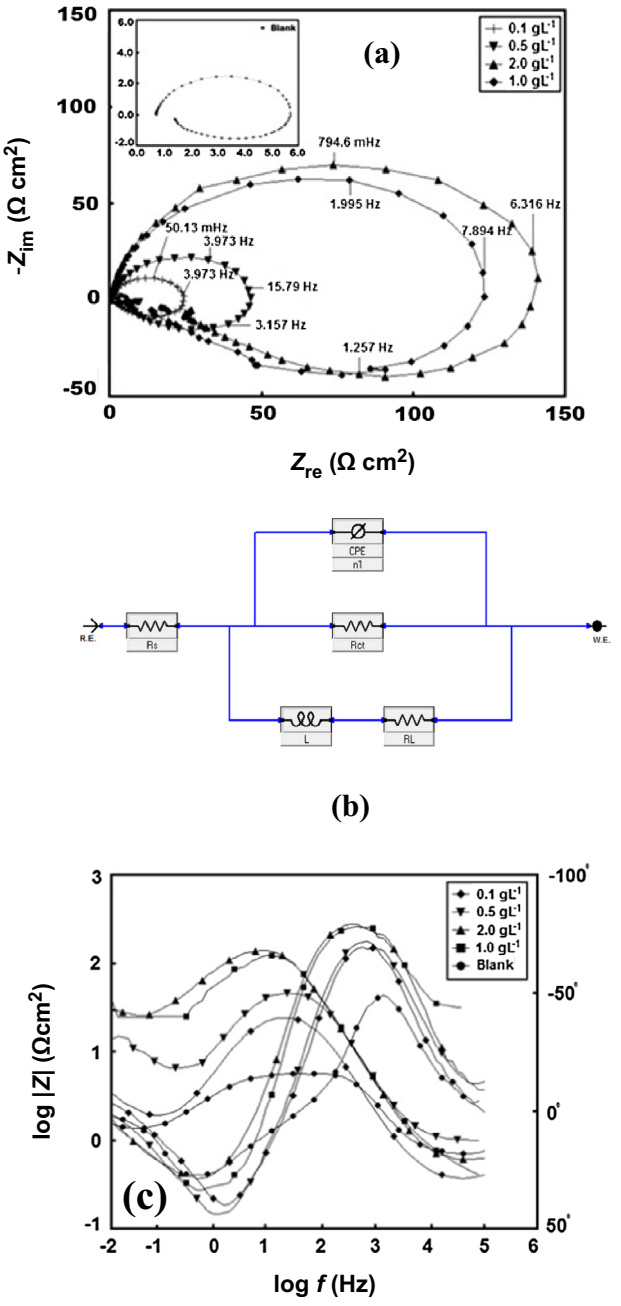

Figure 2 (a) Nyquist plot of AA in 1 M HCl in the absence and presence of different concentrations of PPE at 303 K. (b) Electrical equivalent circuit used for the analysis of impedance spectra. (c) Bode (log f vs. log $|Z|$) and phase angle (log f vs. α) plot of impendence spectra for aluminium in 1 M HCl in the absence and presence of different concentrations of PPE.

frequencies. With the addition of PPE, no changes are found in the shape of spectra and it is maintained throughout all tested concentrations which clearly indicate that corrosion mechanism was not modified due to the inhibitor addition.

To evaluate the data, an equivalent circuit is used (depicted in Fig. 2b). In this circuit, R_s is the solution resistance, R_{ct} is the charge transfer resistance, R_L and L represent the inductive elements and CPE (Q) is the constant phase element. Appearance of L in the presence of investigated inhibitor explains that aluminium is still going to dissolve via charge transfer process on the adsorbed inhibitor aluminium surface [31].

The polarization resistance R_p can be calculated from the following equation:

$$R_P = \frac{R_t \times R_L}{R_t + R_L} \tag{2}$$

Then the inhibition efficiency (η %) is calculated from R_P using the following relation:

$$\eta\ \% = \frac{R_{P(inh)} \times R_P}{R_{P(inh)}} \times 100 \tag{3}$$

where R_P and $R_{P(inh)}$ are charge transfer resistance in the absence and presence of inhibitor, respectively.

Both R_{ct} and R_p values increase significantly with addition of PPE, which explains about slower corrosion of electrode in the presence of inhibitor. As the R_p value increased, there was decrease in the C_{dl} values. Thus effective corrosion resistance was observed to be associated with high R_p and low C_{dl} values (see Table 3).

The double layer is defined as an electrical capacitor when considered between the charged metal surface and the solution. The inhibitor molecule adsorbs on the metal surface and decreases its electrical capacity by displacing the water molecules and adsorbed ions on the surface and it is explained by formation of a protective layer on the electrode surface [32]. Since PPE molecule will electrostatically adsorb on the metal surface, the thickness of this protective layer increases with increase in inhibitor concentration, resulting in a noticeable decrease in C_{dl}.

The double layer capacitance (C_{dl}) values were calculated using the following equation [33]:

$$C_{dl} = Q(\omega_{max})^{n-1} \tag{4}$$

where ω_{max} is the angular frequency at which imaginary element reaches a maximum. In the table, χ^2 parameter is used to describe the precision data. It was observed that χ^2 values are found to be low in each concentration suggesting that the fitted data have good agreement with the experimental data. Besides, the lower n value for uninhibited solution (n = 0.883) describes a surface inhomogeneity occurring from surface metal roughening and/or surface of corrosion products. The values of n lie between 0.885 and 0.966 in the case of inhibited solution.

In the bode spectra, two time constants are evident, namely a middle frequency (MF) time constant and a low frequency (LF) time constants (Fig. 2c). MF time constant attributed to the capacitive behaviour of the air-formed film covering the macroscopic alloy surface whereas LF time constant related to the inductive behaviour accompanied with the degradation of the impedance ($|Z|$) with frequency lowering corresponding to the relaxation process of adsorbed species in the oxide film covering the electrode surface or re-dissolution of the oxide layer surface.

3.3. Adsorption isotherm

It is well known that good inhibition efficiency is the result of the adsorption of inhibitor molecule on the aluminium surface. Adsorption isotherm provides information about the type of interaction is possible on aluminium surface in HCl. Among

Table 3 Electrochemical impedance parameters for AA in 1 M HCl in the absence and presence of different concentrations of PPE at 300 K.

C_{inh} (g L^{-1})	R_s (Ω)	R_{ct} (Ω cm^2)	n	L (H cm^2)	R_L (Ω cm^2)	CPE (μF cm^{-2})	C_{dl} (μF cm^{-2})	R_p	η (%)	χ^2
0.0	0.718	4.96	0.883	0.798	0.889	129.3	456.1	0.745	–	5.7×10^{-3}
0.1	0.766	22.80	0.947	1.128	4.877	26.11	134.1	3.96	81.3	14.4×10^{-3}
0.5	0.789	32.8	0.961	1.908	5.946	20.32	112.0	5.00	85.1	26.6×10^{-3}
1.0	0.316	78.6	0.885	1.57	17.56	10.20	81.23	12.1	94.5	92.8×10^{-3}
2.0	0.598	80.3	0.966	2.72	20.51	7.21	50.06	16.3	95.5	14.4×10^{-3}

various isotherms (Frumkin, Langmuir, Temkin, Freundlich, Bockris–Swinkels and Flory–Huggins), Langmuir adsorption isotherm was found to be the best description in our present study, which is represented by the following equation [34]:

$$\frac{C_{inh}}{\theta} = \frac{1}{K_{ads}} + C_{inh} \tag{5}$$

where K_{ads} is the adsorption equilibrium constant, C denotes the concentration of the inhibitor and θ is surface coverage value. By plotting the log C_{inh}/θ vs. C_{inh}, a straight line is observed in Fig. 3, which indicates the adsorption of inhibitor molecule on the metal surface obeys Langmuir adsorption isotherm.

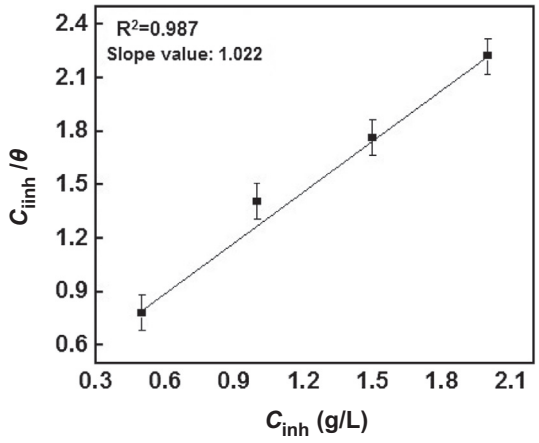

Figure 3 Langmuir's isotherm plot for adsorption of PPE molecule on aluminium in 1 M HCl.

The values of K_{ads} are in association with the standard Gibbs free energy of adsorption $\Delta G^0_{(ads)}$ by the following equation [35].

$$K_{ads} = \frac{1}{C_{(sol.)}} \exp\left(\frac{-\Delta G^0_{ads}}{RT}\right) \tag{6}$$

where $C_{solvent}$ is the concentration of water in solution, R is universal gas constant and T is the absolute temperature. It should be noted that the concentration of water is taken here in g L^{-1} with the approximate value of 1.0×10^3 g L^{-1} (in the place of 55.5 mole/L) and also the unit of K_{ads} is showing in g^{-1} L.

The linear regression (0.987) and slope value (1.022) are observed for PPE. It can be clearly seen in Fig. 3 that slope value is 1 and linear correlation coefficients (r) are close to 1, suggesting the adsorption of inhibitor molecule on aluminium surface obeys Langmuir adsorption isotherm. According to the literature, if the values of standard Gibbs free energy of adsorption are near to the −20 kJ mol^{-1} or lower (more positive), interaction was found to be electrostatic between the adsorbent and adsorbate (physisorption), while those close to −40 kJ mol^{-1} or higher (more negative) indicates sharing or charge transfer from the inhibitor molecules to the metal surface to form a coordinate type bond, i.e. chemisorption. In our case, the calculated value of ΔG_{ads} is −27.34 kJ mol^{-1} for studied PPE and this value pointed out the adsorption of compounds occurs by chemisorption as well as physisorption.

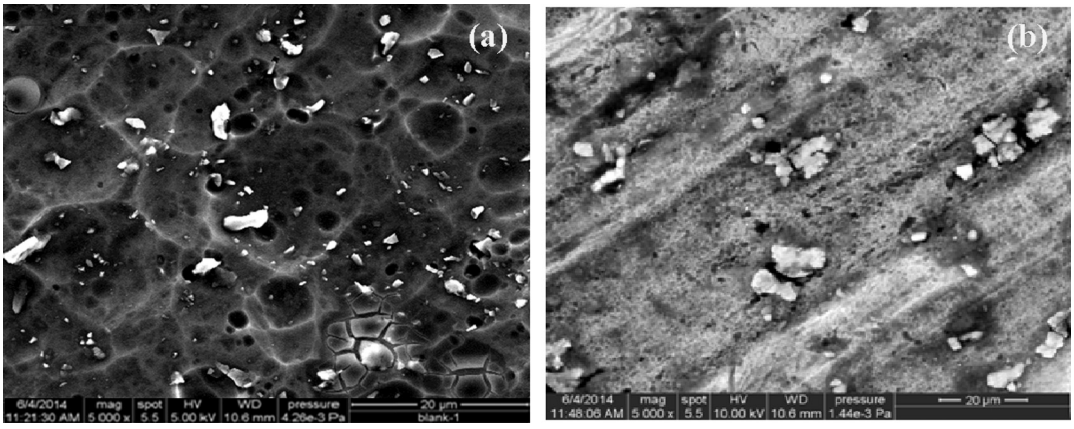

Figure 4 SEM micrographs of (a) uninhibited and (b) inhibited AA sample containing 2.0 g L^{-1} of PPE in 1 M HCl.

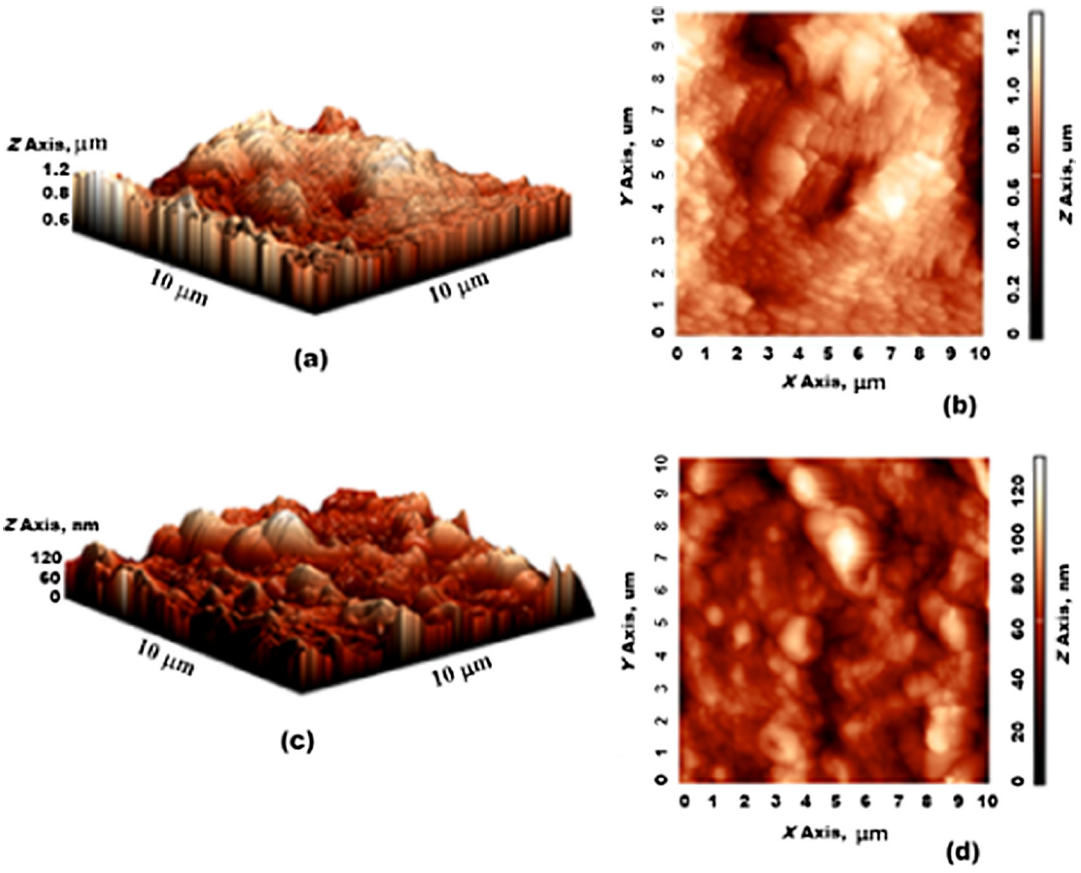

Figure 5 AFM images of aluminium specimens. (a–b) Uninhibited 3D and 2D micrographs and (c–d) inhibited 3D and 2D micrographs.

3.4. Surface analysis

3.4.1. Scanning electron microscopy

The SEM images of AA in 1 M HCl without and with the addition of inhibitor are displayed in Fig. 4. Fig. 4a shows the SEM micrograph of the uninhibited AA surface which reveals that surface was damaged with clearly visible cracks and pits. Fig. 4b displays the AA surface after the corrosion test in the presence of PPE at 2.0 g L^{-1}. It presents a smooth and clean surface in comparison with uninhibited AA surface, which indicates that the adsorbed inhibitor molecule of PPE inhibits the corrosion of AA in HCl.

3.4.2. Atomic force microscopy

Further investigation of the corrosion inhibition ability of the extract was carried out by means of AFM in order to characterize the AA surface microstructure. Fig. 5(a–d) depicts three-dimensional and two-dimensional AFM images of AA surface after 3 h exposure in uninhibited and inhibited system at 303 K. In uninhibited system, the AA surface was fairly damaged due to dissolution in corrosive medium (Fig. 5a) with maximum height scale of 1.2 µm. The maximum height scale

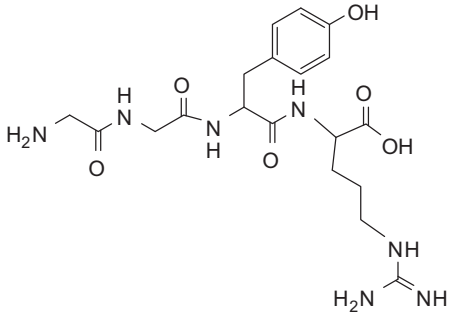

Figure 6 Molecular structure of Papain molecule.

Table 4 AFM data obtained from height profile for aluminium surface immersed in inhibited and uninhibited environment.

Samples	RMS (Sq) Roughness (µm)	Average (Sa) Roughness (µm)	Area (St) Peak-to-valley height (µm)
Aluminium metal immersed in 1 M HCl solution	0.312	0.246	2.876
Metal immersed in 1 M HCl solution containing PPE	0.020	0.015	0.137

of inhibited AA surface (Fig. 5c) was 120 nm due to formation of a protective layer on surface which causes the decrease in AA surface roughness and effectively protects AA from corrosion.

A three dimensional roughness data were also obtained with AFM techniques, in which the value of root-mean-square roughness (Sq), average roughness (Sa) and St (the maximum peak-to-valley height) for aluminium metal surface in the absence and presence of PPE are shown in Table 4. In uninhibited system, the values of Sa, Sq and P-V height are greater (given in Table 4) because of the greater surface roughness of AA. It may be attributed to the dissolution of oxide film layer but the values significantly reduced by the addition of 2.0 g L^{-1} of PPE (Table 4). These parameters confirmed about smoother surface due to the formation of a compact protective film on the metal surface thereby inhibiting the corrosion of aluminium metal.

3.5. Quantum chemical study

Quantum chemical calculations were used to investigate the adsorption and inhibition effect of studied inhibitor molecule. Papain was found to be major constituent given in Fig. 6 that is responsible for the inhibition action of PPE. DFT calculation was used to understand a better mechanism of adsorption in both neutral and protonated forms of Papain on the aluminium corrosion.

3.5.1. Neutral form of inhibitor

The values of calculated quantum chemical parameters such as E_{HOMO}, E_{LUMO}, ΔE (E_{LUMO}–E_{HOMO}) and μ are listed in Table 5. The optimized structure, HOMO and LUMO of neutral papain is shown in Fig. 7a–c.

Frontier orbital theory is very helpful in determining the adsorption centres of the inhibitor molecule and also responsible for an interaction between the frontier orbital (HOMO and LUMO) of reacting species. However, E_{HOMO} and E_{LUMO} are electronic parameters associated with the tendency to donate and accept electrons respectively. Increasing in the value of E_{HOMO} suggests lower value of ionization potential and therefore, electrons are easily donated and facilitate the adsorption process and lower value of E_{LUMO} shows higher tendency of molecule to accept electrons [36].

The difference in energy level (ΔE) is an important factor and considered in the evaluation of inhibition potential. Smaller value of the energy difference (ΔE) between the participating HOMO and LUMO leads to easier polarization of the molecule which results in higher inhibition efficiency and it is due to the fact that the energy required to remove an electron from the last occupied orbital will be low.

The better action of electron donation mainly depends on the large negative charges on atoms. By doing detailed study of Mulliken charges, the large negative value is found in case of N_{28}, which can donate its lone pair electron to the empty metal orbital due to which the papain molecule could be adsorbed on the metal surface.

In the neutral form of inhibitor the HOMO is associated on N_{28} and O_{26} atoms, which suggests that these are the sites which donate electrons to the metal empty orbitals. Also LUMO is associated with benzene ring, which reveals that this site would accept electron from the filled metal orbitals.

Table 5 Mulliken charges of heteroatoms.

Mulliken charges of heteroatoms															
	N_{10}	N_{16}	N_{18}	N_{19}	N_{21}	N_{24}	N_{28}	O_{13}	O_{15}	O_{20}	O_{26}	O_{29}	O_{30}	Dipole (μ)	E_{HOMO} (Hartree)	E_{LUMO} (Hartree)	ΔE (Hartree)
Papain	−0.671	−0.661	−0.743	−0.570	−0.664	−0.674	−0.770	−0.563	−0.381	−0.444	−0.430	−0.509	−0.646	4.866	−0.175	−0.022	0.153
$Papain^{+}$	−0.677	−0.661	−0.741	−0.577	−0.663	−0.642	−0.717	−0.561	−0.379	−0.429	−0.402	−0.486	−0.639	29.464	−0.040	0.020	0.06

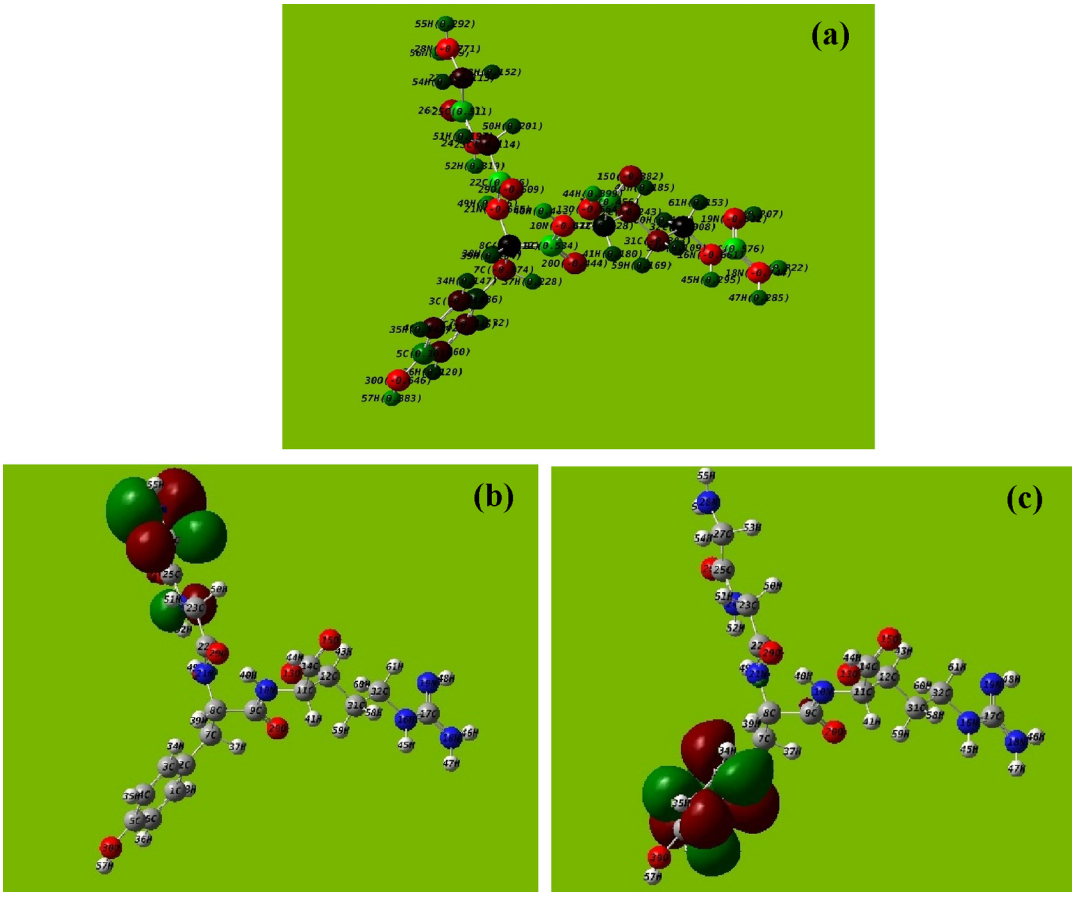

Figure 7 (a) Optimized molecular structure, (b) HOMO and (c) LUMO of neutral Papain molecule.

3.5.2. Pronated form

In the aqueous medium, the corrosion inhibition chemistry of PPE has been changed. PPE is found to be very much susceptible for protonation by involving the lone pair of electrons present on heteroatoms. However, N_{28} is the heteroatom having large negative value of Mulliken charge and therefore protonation occurs by this site. The protonated species optimized structure; HOMO and LUMO are shown in Fig. 8a–c. After observing the HOMO and LUMO, it can be said that benzene ring acts as an electron donor and O_{13} and O_{15} are the acceptor sites in aqueous acidic medium. The electronic parameters of protonated molecule are given in Table 5.

It is found that E_{HOMO} value is higher in aqueous phase (protonated) than that in neutral species, which indicates that in aqueous medium protonated PPE has greater tendency for donation of electrons than neutral one. So, protonated species would bind more strongly to the metal surface as compared to the neutral species. Also ΔE value in protonated species is lower than in neutral species, which further suggest that protonated one is more reactive than neutral one. This further confirms that both physical and chemical adsorptions of inhibitor molecules occur on metal surface. No significant relationship has been found between the dipole moment values and inhibition efficiencies. Besides, there is a lack of agreement in the literature on the correlation between the dipole moment and inhibition efficiency [37–40].

3.6. Mechanism of inhibition

The adsorption mechanism of papain molecule on AA surface depends upon its molecular structure that contains heteroatoms such as, nitrogen and oxygen and delocalized π-electrons of heterocyclic ring and a protonated species [41].

There are various active sites for adsorption in PPE. Thus following adsorption and inhibition mechanism are proposed involving inhibitor molecule on metal surface (Fig. 9). In acidic solution, inhibitor molecule becomes protonated by accepting protons:

$$[\mathrm{PPE}] + \mathrm{H}^{+} \leftrightarrow [\mathrm{PPE}]^{+}$$

Due to specific adsorption and small degree of hydration, chloride ions (Cl^{-}) firstly adsorbed on the positively charged metal surface and thus, create an excess negative charge towards the solution side of the metal and favour more adsorption of cations. Thus an electrostatic interaction (physical adsorption) is created between the protonated (PPE^{+}) molecule and an excess negative charge towards the metal surface through which they form a protective layer. Furthermore, in aqueous medium, the protonated species start competing with H^{+} ions for electrons on metal surface. Thus, the cationic form of inhibitor molecule returns to its neutral form after releasing of H_2 gas and lone pairs present on heteroatoms in molecule is transferred to the vacant p orbital of aluminium and thus promotes chemical adsorption [42].

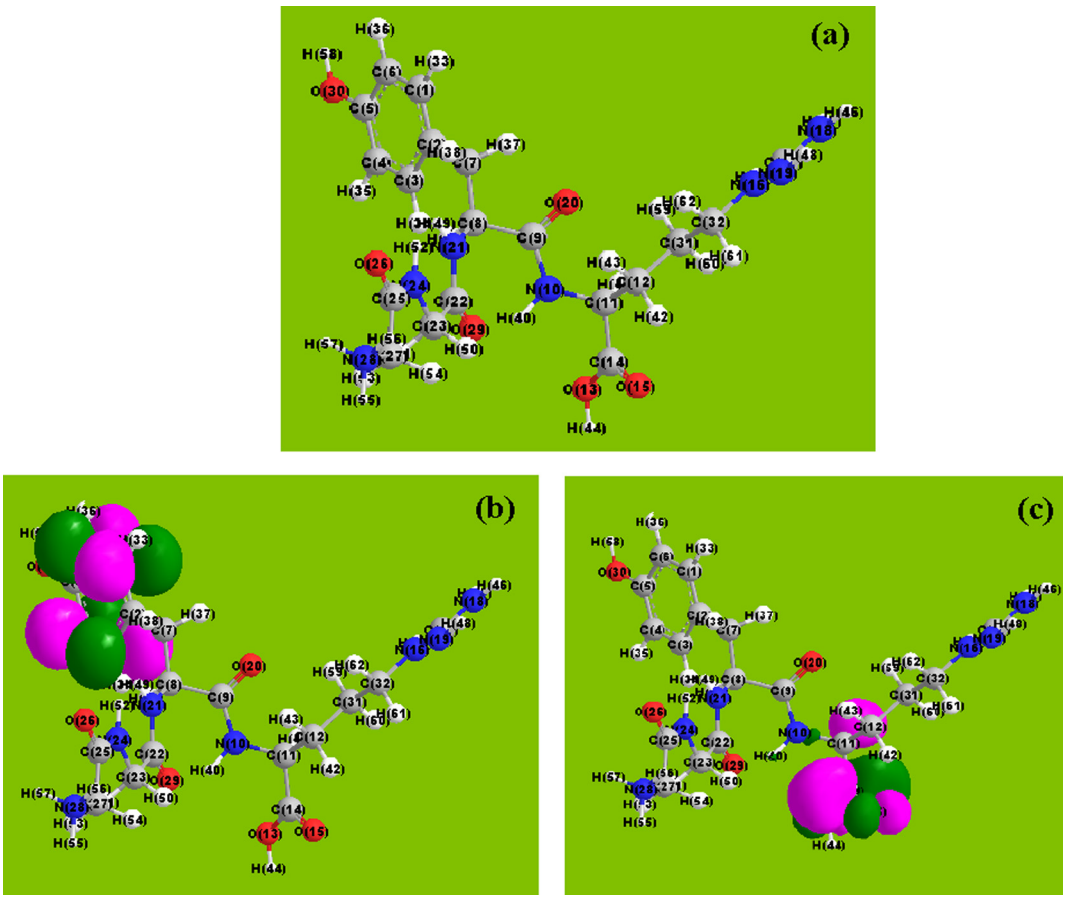

Figure 8 (a) Optimized molecular structure (b) HOMO (c) LUMO of protonated Papain molecule.

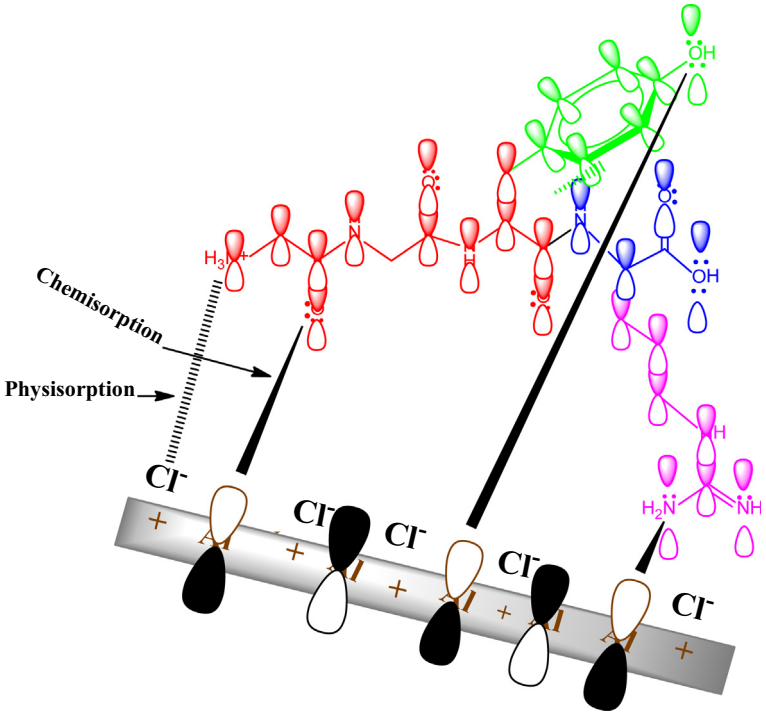

Figure 9 Schematic representation of the adsorption behaviour of inhibitor molecule on aluminium surface in 1 M HCl.

4. Conclusion

1. Aqueous extract of Papaya peel is an environmentally benign good corrosion inhibitor for AA in HCl. Inhibition efficiency increases with increasing the concentration of extracts.
2. Tafel polarization indicates that PPE is arranged as cathodic type inhibitor.
3. EIS indicates that increase in R_{ct} and decrease in C_{dl} are observed which is explained by decrease in local dielectric constant and/or an increase in the electrical double layer thickness due to the adsorbed inhibitor molecules at the metal/solution interface.
4. Adsorption of the PPE on the AA surface in HCl obeys the Langmuir's isotherm.
5. The SEM and AFM analysis showed the formation of a protective film on the AA surface in inhibited system.
6. Quantum chemical approach is adequately sufficient to predict the structural and molecular suitability to be an inhibitor.

Acknowledgement

Authors are highly thankful to Prof. V.B. Singh, Head (Department of chemistry), B.H.U., for providing SEM and AFM facilities for successful completion of my research work.

References

[1] Prabhu D, Rao P. J Environ Chem Eng 2013;1:676–83.
[2] Garrigues L, Pebere N, Dabosi F. Electrochim Acta 1996;41:1209–15.
[3] Abd El Haleem SM, Abd El Wanees S, Abd El Aal EE, Farouk A. Corros Sci 2013;68:1–13.
[4] Awad MK, Metwally MS, Soliman SA, El-Zomrawy AA, bedair MA. Ind Eng Chem 2014;20:796–808.
[5] Khaled KF, Al-Qahtani MM. Mater Chem Phys 2009;113:150–8.
[6] Ehsani A, Nasrollahzadeh M, Mahjani MG, Moshrefi R, Mostaanzadeh H. Ind Eng Chem 2014;20:4363–70.
[7] Rethinnagiri V, Jeyaprakash P, Arunkumar M, Maheswaran V, Madhiyalagan A. Adv Appl Sci Res 2012;3:1718–26.
[8] Umoren SA, Obot IB, Israel AU, Asuquo PO, Solomon MM, Eduok UM, Udoh AP. Ind Eng Chem 2014;20:3612–22.
[9] Deng S, Li X. Corros Sci 2012;64:253–62.
[10] Abd-El-Naby BA, Abdullatef OA, El-Kshlan HM, Khamis E, Abd-El-Fatah MA. Port Electrochim Acta 2015;33:1–11.
[11] Jain T, Chowdhary R, Mathur SP. Mater Corros 2006;57:422–6.
[12] Abiola OK, Oforka NC, Ebenso EE, Nwinuka NM. Anti Corros Method Meter 2007;54:219–24.
[13] Ating EI, Umoren SA, Udousoro II, Ebenso EE, Udoh AP. Green Chem Lett Rev 2010;3:61–8.
[14] Odewunmi NA, Umoren SA, Gasem ZM. J Environ Chem Eng 2015;3:286–96.
[15] Saleh RM, Ismail AA, El Hosary AA. Br Corros J 1982;17:131–5.
[16] Adejo SO, Gbertyo JA, Ahile JU, Gabriel Tyohemba T. IJSER 2013;4:2308–13.
[17] James O, Akaranta O. Afr J Pure Appl Chem 2009;3:262–8.
[18] Ukpe RA, Odoemelam SA, Odiongenyi AO, Eddy NO. J Bioprocess Chem Eng 2014;2:2348–3768.
[19] Chaiwut P, Nitsawang S, Shank L, Kanasawud P. Chiang Mai J Sci 2007;34:109–18.
[20] Yadav DK, Quraishi MA. Ind Eng Chem Res 2012;51:14966–79.
[21] Ashassi-Sorkhabi H, Shabani B, Aligholipour B, Seifzadeh D. Appl Surf Sci 2006;252:4039–47.
[22] Li XH, Deng SD, Fu H. Corros Sci 2011;53:1529–36.
[23] Li X, Deng S, Xie X. J Taiwan Inst Chem 2014;45:1865–75.
[24] Khaled KF, Al-Qahtani MM. Mater Chem Phys 2009;113:150–8.
[25] Amin MA, Mohsen Q, Hazzai OA. Mater Chem Phys 2009;114:908–14.
[26] Lenderink HJW, Linden MVD, De Wit JHW. Electrochim Acta 1993;38:1989–92.
[27] Noor EA. Mater Chem Phys 2009;114:533–41.
[28] Valand T, Heusler KE. J Electroanal Chem 1983;149:71–82.
[29] Singh AK, Quraishi MA. Corros Sci 2010;52:152–60.
[30] Abd El Rehim SS, Hassan HH, Amin MA. Mater Chem Phys 2001;70:64–72.
[31] Amin MA, Khaled KF, Mohsen Q, Arida HA. Corros Sci 2010;52:1684–95.
[32] McCafferty E, Hackerman N. J Electrochem Soc 1972;119:146–54.
[33] Umoren SA, Obot IB, Ebenso EE, Okafor PC. Anti-Corros Meth Mater 2006;53:277–82.
[34] Ramya K, Mohan R, Anupama KK, Joseph A. Mater Chem Phys 2015;149–150:632–47.
[35] yadav DK, Quraishi MA, Maiti B. Corros Sci 2012;55:254–66.
[36] Ansari KR, Quraishi MA. Inst J Taiwan Chem 2015;54:145–54.
[37] Gao G, Liang C. Electrochim Acta 2007;52:4554–9.
[38] Khalil N. Electrochim Acta 2003;48:2635–40.
[39] Rodrigez-Valdez LM, Martinez-Villafane A, Glossman-Mitnik D. J Mol Struct (THEOCHEM) 2005;713:65–70.
[40] Yadav DK, Maiti B, Quraishi MA. Corros Sci 2010;52:3586–98.
[41] Fouda AS, Abdallah M, Mohamed TY, Fouad E. Prot Met Phys Chem Surf 2011;47:803–12.
[42] Li X, Deng S. Corros Sci 2012;65:299–308.

Namrata Chaubey is a research scholar, doing PhD from Udai Pratap (Autonomous) College, Varanasi under the supervision and co supervision of Dr. Vinod Kumar Singh and Prof. M. A. Quraishi respectively.

Vinod Kumar Singh is an associate professor in Udai Pratap (Autonomous) College, Varanasi. He has been completed his PhD from Department of Chemistry, BHU. His area of interest is corrosion and green chemistry.

I am presently serving as Professor and Head Department of Chemistry in Indian Institute of Technology (Banaras Hindu University). I obtained B.Sc. (1969) degree and M.Sc. (1971) degree from Saugar University, Saugar, and M.Phil (1978) and Ph.D (1986) from Kurukshetra University. D.Sc. (2004) from centrally funded AMU Aligarh. Before joining as Professor at BHU, I was Reader (1990–2005) at AMU Aligarh.